Egypt. J. Chem. **Vol. 67**, No. 12 pp. 129 - 141 (2024)

Egyptian Journal of Chemistry

http://ejchem.journals.ekb.eg/

New Nanoparticle Metal Complexes Based on Cefaclor and 2,2′-Bipyridineligands: Synthesis, Characterization, DFT Studies and Their Antimicrobial Evaluation

H. A. Abdallah, S. A. Sadeek*, M. M. Zareh, M. S. El-Attar, W. A. Zordok, B.Abd El-Wahaab

Department of Chemistry, Faculty of Science, Zagazig University, Zagazig, 44519, Egypt

Abstract

Five new nanoparticles mixed ligand complexes were synthesized by interacting the antibiotic cefaclor**(CEF)** with some metal ions such as Cr(III), Co(II), Cu(II), Zn(II) and Cd(II) with 2,2′-bipyridine **(Bipy)** in 1:1:1 molar ratio. The complexes were characterized by elemental analyses, thermal analyses (TG, DTG, and DTA), spectroscopic methods (FT-IR, UV-Vis, ^{1}H NMR, and X-ray powder diffraction, or XRD), molar conductivity and magnetic moment (μ_{eff}). The molar conductance data supported that all complexes were electrolyte in nature with 1:2 for Cr(III) and 1:1 for bivalent metal ions. Magnetic moments data and electronic absorption spectra for all complexes supporting octahedral geometry for the metal complexes. Infrared data showed that **CEF** interacted as a tridentate ligand with metal ions via nitrogen of primary amine, one oxygen atom of carboxylate group and carbonyl group of a β-lactam ring, while, **Bipy** chelated through two nitrogen atoms. Optical band energy gap (E_g), the calculated values of E_g for the metal complexes confirmed they were semiconductors. **CEF**, **Bipy**, and their metal complexes underwent TG and DTG, and the decomposition mechanisms were discussed. DTA data exhibit exothermic and endothermic peaks. The average crystalline size (C_s), dislocation density (D), full width at half maximum (FWHM), and the kind of compounds (crystalline or amorphous) were determined using XRD which indicted that complexes **(3)**, **(4)** and **(5)** were crystalline but complexes **(1)** and **(2)** were amorphous in nature. The compounds' optimal molecular geometry was determined using density functional theory (DFT) computations. All studied complexes with σ values varied from 22.222 to 44.444 eV were soft respect to **CEF** (σ = 16.393 eV). All compounds were tested for their antimicrobial activities against gram-positive and gram-negative strains of bacteria and fungi. The results indicated that the tested metal complexes exhibited notable effectiveness more than **CEF** and **Bipy,** of which these synthesized compounds could potentially serve as improved bactericides and fungicides.

Keywords: cefaclor, 2,2′-bipyridine, metal complexes, characterization, antimicrobial investigation;

1. INTRODUCTION

Cephalosporins are β-lactam antibiotics, which are among the oldest and most widely used naturally occurring antimicrobial drugs. The important intermediary in the semisynthetic manufacture of a significant number of cephalosporins is 7-aminocephalosporanic acid, which is created by the hydrolysis of cephalosporin produced via fermentation [1-5]. Cephalosporins are physically and pharmacologically linked to penicillin, which has a β-lactam ring structure that inhibits bacterial cell wall formation, and so are bactericidal [6-9]. β-lactam antibiotic drugs easily interact with metal ions forming metal complexes which accelerate the rates of drug absorption through the membranes [6,7]. The interactions of drugs with metal ions were especially studied because of their interesting biological and chemical properties [10-12]. Inorganic biological metal ions provide a variety of important functions in biological and pharmaceutical sciences [10-15]. Based on their wide spectrum of coordination numbers and geometries as well as kinetic properties, metal compounds enable unique mechanisms of drug action that cannot be realized by organic agents [10-12].

*Corresponding author e-mail: s_sadeek@zu.edu.eg.; (Sadeek A. Sadeek).
EJCHEM use only: Received date 13 March 2024; revised date 17 May 2024; accepted date 02 June 2024
DOI: 10.21608/ejchem.2024.276743.9452

Cefaclor (CEF) (Scheme 1A) is a broad spectrum antibacterial agent and is a unique antibiotic that belongs to the second category of cephalosporin antibiotics which is commonly used against G+ve, G-ve bacterial. Also, CEF used to treat certain infections caused by bacteria such as pneumonia and ear, lung, skin, throat and urinary tract infections [16,17]. CEF drug contains common donor atoms such as nitrogen, oxygen and sulphur, which easily coordinate with metal ions to form complexes [16-18]. Three distinct donation sites in cefaclor (C=O) β-lactam, (C=O) carboxylic acid, and (-NH) amine groups are present and appropriate for chelation [16-18].

2,2′-bipyridine (Bipy) (Scheme 1B) chelated as a bidentate ligand with metal ions through two nitrogen donor atoms [10,15]. Bipy complexes were used in the field of catalysis, supramolecular, material chemistry, analytical chemistry, biology, and energy transfer [19]. In the literature survey, numerous mixed metal complexes, including Bipy and various other donor ligands, have been documented in published literature [10,15, 20-23]. A previous literature research proves that no work has been reported on CEF in the presence of Bipy, and therefore, the aim of the present work is to synthesize some new nanoparticles mixed ligand complexes of inorganic metal ions such as Cr(III), Co(II), Cu(II), Zn(II), and Cd(II) with CEF with Bipy. The new metal complexes were characterized by elemental analysis, FT-IR, UV-Vis., 1H NMR, XRD, DFT, magnetic measurements, thermal analysis, and molar conductivity. Also, CEF efficiency in the new form was evaluated against some bacterial and fungal strains.

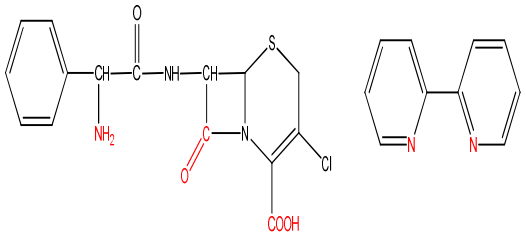

Scheme 1: CEF (A) and Bipy (B)

2. EXPERIMENTAL

2.1 | Materials

All of the analytical-grade chemicals and solvents used for this investigation were used as received. CEF, Bipy(99.5%), absolute ethanol (99.8%), CrCl3.6H2O (98%), $CoCl_2$ (98%), $CuCl_2$ (97%), $ZnCl_2$ (98%), and $CdCl_2$ (99%) were purchased from Sigma and Aldrich Chemical Co.

2.2 | Synthesis of metal complexes

Brown solid complex $[Cr(CEF)(Bipy)(H_2O)]Cl2.3H_2O$ (1), green solid complex $[Co(CEF)(Bipy)(H_2O)]Cl.2H_2O$ (2), faint green solid complex $[Cu(CEF)(Bipy)(H_2O)]Cl.H_2O$ (3), pale yellow solid complex $[Zn(CEF)(Bipy)(H_2O)]Cl.2H_2O$ (4) and buff solid complex $[Cd(CEF)(Bipy)(H_2O)]$ $Cl.5H_2O$ (5) were synthesized by adding 2 mmol (0.735 g) of CEF in 30 mL of ethanol in presence of 2 mmol (0.312 g) Bipy to 2 mmol of $CrCl_3.6H_2O$, $CoCl_2$, $CuCl_2$, $ZnCl_2$, and $CdCl_2$ dissolved in 20 mL ethanol with 1:1:1 (CEF:M:Bipy) molar ratio. The mixture was refluxed upon stirring for six hours and the solid precipitate was formed upon evaporation at room temperature for seven days, the precipitate was dried under vacuum over anhydrous calcium chloride.

2.3 | Instruments

The determination of CHN percentages was performed using an elemental analyzer, specifically the PerkinElmer 2400 instrument. Metal ions fractions were detected using atomic absorption technique and thermogravimetric analysis [10,15]. Utilizing an FTIR 460 PLUS Spectrophotometer, FT-IR spectra in 4000 to 400 cm-1 region of KBr discs were done. Under N2 as the environment and temperature range 25-1000 °C using alumina crucibles, thermal studies were carried out utilizing a Shimadzu TGA-50H thermal analyzer. UV3101PC Shimadzu was used to find the electronic absorption spectra. 1H NMR spectra in dimethyl sulfoxide (DMSO-d_6) were recorded on Varian Mercury VX-300 NMR spectrometer with tetra methyl saline (TMS) as reference. μeff of the complexes was done using Gouy balance which calibrated with $Hg[Co(SCN)_4]$. At concentration solutions (1×10-3 M) in DMF, CONSORT K410 was used to evaluate the molar conductance of the compounds. Melting points of the examined complexes were noted using Buchi apparatus. XRD was done using a diffract meter (analytical XPERT PRO MPD). Cu-Kα radiation (λ = 1.5418 Å) was used at a rate of 40 kV and 40 mA. Every measurement was conducted using freshly made solutions at room temperature.

2.4 | Antimicrobial assay

In vitro antimicrobial activity of CEF, Bipy and the complexes were dissolved in DMSO at a concentration of 1 mg/mL and subjected to the disc diffusion technique, which was performed using a modified version of Beecher and Wong's previously established method [24,25] against two Gram positive Staphylococcus aureus (S. aureus), Straptococcusmutans (S. mutans) and two Gram negative Escherichia coli (E. coli), Klebsiella pneumonia (K. pneumonia) was evaluated, these strains were aseptically collected from Microbial Wealth Center Ain Shams University in order to represent bacteria. Also, the antifungal activity of the compounds was assessed against Candida albicans (C. albicans) and Aspergillusniger (A. niger) using Sabouraud dextrose agar medium. Ampicillin and Gentamicin, widely used as standard drugs for G+ve and G-ve bacteria were included in the study. Nystatin as standard drug for fungal strains and DMSO as solvent control were used. The compounds were tested against both fungal and bacterial strains at concentration 15 mg/mL.

The sterilized liquid substance was carefully poured onto the sterilized circular plates (measuring 20-25 mm in diameter). After pouring, each plate was left undisturbed at room temperature until it solidified. A suspension of microorganisms was prepared in sterilized saline solution, which was equivalent to a McFarland 0.5 standard solution (containing approximately 1.5x 105 colony-forming units per milliliter). The opacity of the suspension was modified to an optical density (OD) of 0.13 at a wavelength of 625 nm using a spectrophotometer. Ideally, within 15 minutes of adjusting the turbidity, a sterile cotton swab was immersed in the adjusted suspension and spread evenly on the dried agar surface. The swab was then left to dry for 15 minutes with the lid of the container in place. To create wells for subsequent experiments, a sterile borer was used to make holes with a diameter of 6 mm in the solidified agar. Using a micropipette, 100 µL of the compound being tested was added to each well. The plates were then placed in an incubator at a temperature of 37 °C for duration of 24 hours, specifically for assessing antibacterial activity [26]. This experiment was conducted in three independent repetitions, and the zones of inhibition were measured in millimeters. The percentage of activity index for the tested compounds was determined using eq. (1) [27].

$$\%\ \text{Activity index} = \frac{\text{Inhibition zone by test compound diameter}}{\text{Inhibition zone by standard diameter}} \times 100 \quad (1)$$

3. RESULTS AND DISCUSSION

3.1 Elemental and molar conductance

The physical and analytical information of CEF, Bipy and their metal complexes were tabulated in Table 1. According to the microanalysis data for all synthesized complexes, the molecular formulas were elucidated with molar ratio 1:1:1 (CEF: M: Bipy). For metal complexes, the values of molar conductance ranged from 75.67 to 144 Ω cm2 mol^{-1} which indicated that all complexes were electrolyte with 1:2 for Cr(III) and 1:1 for other bivalent metal complexes[10,11,28]. All tested complexes give a white precipitate with silver nitrate solution, this prove the presence of chloride ions as counter ion which good agree matching with the molar conductivity values.

3.2 | FT-IR spectra and mode of chelation

FT-IR analysis was performed on the compounds CEF, Bipy, and their respective metal complexes. The resulting spectra were presented in Figure S1, the significant bands were identified and their corresponding data were listed in Table 2. A comparison was made between the spectra of the complexes and those of CEF and Bipy in order to determine the coordination sites involved in the chelation process. In the spectrum of CEF, specific bands at 3323, 1756, and 1697 cm^{-1} were observed, which could be attributed to the vibrations of the amine group (ν(N-H) amine), the β-lactam carbonyl group (ν(C=O)β-lactam), and the carboxylic carbonyl group (ν(C=O)carboxylic), respectively [29]. The position of these peaks were shifted after complex formation with CEF, the band corresponding to ν(C=O) of carboxylic group which located at 1697 cm^{-1}disappeared in all complexes and new bands appeared in the region 1603- 1642 cm^{-1} for νas(COO-) and in the region 1339-1438 cm^{-1} for νs(COO-) with Δν> 200 cm^{-1} which indicated carboxylic group coordinated as monodentate through one oxygen atom [10,11,29]. Also, the ν(C=O) lactam band at 1756 cm^{-1} in the spectrum of CEF is shifted to lower values in the spectra of complexes at around 1663 cm^{-1} supporting the coordination of CEF through oxygen of lactam carbonyl group rather than amide carbonyl group, where the shift was not significant [29]. The shift of

Table 1: Analytical and physical data for **CEF, Bipy** and their metal complexes

Compounds M.Wt. (M.F.)	Color Yield (%)	M.P. (°C)	Found (Calc.) (%)					Λ Ω $cm^2 mol^{-1}$
			C	H	N	M	Cl	
CEF 367.45 ($C_{15}H_{14}N_3O_4SCl$)	Pale yellow -	327	-	-	-	-	-	-
Bipy 156.00 ($C_{10}H_8N_2$)	White -	70	-	-	-	-	-	4.12
(1) 717.34 ($CrC_{25}H_{29}N_3O_8SCl_3$)	Brown 95.02	238	41.74 (41.82)	4.00 (4.04)	9.70 (9.76)	7.15 (7.25)	14.71 (14.83)	144.00
(2) 670.83 ($CoC_{25}H_{27}N_3O_7SCl_2$)	Green 88.34	110	44.62 (44.72)	3.91 (4.02)	10.31 (10.43)	8.70 (8.78)	10.44 (10.57)	75.67
(3) 657.44 ($CuC_{25}H_{25}N_3O_6SCl_2$)	Faint green 92.32	142	45.40 (45.63)	3.75 (3.80)	10.51 (10.65)	9.54 (9.66)	10.66 (10.79)	77.23
(4) 677.31 ($ZnC_{25}H_{27}N_3O_7SCl_2$)	Pale yellow 75.56	260	44.15 (44.29)	3.91 (3.99)	10.25 (10.34)	9.57 (9.65)	10.34 (10.47)	79.55
(5) 778.31 ($CdC_{25}H_{33}N_3O_{10}SCl_2$)	Buff 70.44	188	38.42 (38.55)	4.18 (4.24)	8.87 (8.99)	14.32 (14.44)	9.06 (9.11)	76.85

Table 2: Significant IR frequencies (cm^{-1}) for **CEF, Bipy** and their metal complexes

Compounds	ν(O-H)	ν(N-H); amine	ν(C=O); β-lactam	ν(C=O); COOH	$\nu_{as}(COO^-)$	ν(C=N); Bipy	$\nu_s(COO^-)$	ν(M-O), ν(M-N)
CEF	3400w	3323m	1756vs	1697s	-	-	-	-
Bipy	3440mbr	-	-	-	-	1578ms	-	-
(1)	3410w	3336w	1661vs	-	1603ms	1530m	1339m	601w, 551w
(2)	3405w	3225w	1662vs	-	1604s	1564w	1397m	616w, 515w
(3)	3407w	3202w	1647vs	-	1601s	1566m	1400w	697m, 575m
(4)	3408w	3275m	1670vs	-	1615w	1564m	1398sh	651s, 538w
(5)	3411w	3342w	1669vs	-	1622w	1564ms	1415s	659s, 524w

Keys: s=strong, w=weak, v=very, m=medium, br=broad, ν=stretching

Table 3: Ultraviolet-visible spectra for **CEF, Bipy** and their metal complexes

Compounds	Peak nm	Peak cm^{-1}	Assignment	ε* $(M^{-1}cm^{-1})x\ 10^3$	10Dq cm^{-1}	10Dq kJ/mol	CFSE	μeff (B.M)
CEF	295 320,390	33898 31250,25641	π→π* n→π*	0.032 0.052,0.011	-	-	-	-
Bipy	284 347	35211 28818	π→π* n→π*	1.839 1.789	-	-	-	-
(1)	296 320,385 460 521	33783 31250,25974 21739 19193	π→π* n→π* LMCT d-d transition	0.030 0.064,0.036 0.018 0.004	19193	229	-274	3.7
(2)	296 380 445 505	33783 26315 22471 19801	π→π* n→π* LMCT d-d transition	0.033 0.098 0.018 0.005	19801	237	-190 + 2P	1.8
(3)	295 320,380 455 506	33898 31250,26315 21978 19762	π→π* n→π* LMCT d-d transition	0.031 0.077,0.077 0.006 0.002	19762	236	-142 + 4P	1.73
(4)	295 310, 380 420	33898 32258,26315 23809	π→π* n→π* LMCT	0.028 0.015,0.020 0.011	-	-	-	-
(5)	295 310,340, 375 435	33898 32258, 29412, 26666 22989	π→π* n→π* LMCT	0.030 0.038, 0.025, 0.041 0.023	-	-	-	-

ν(N-H) at 3323 cm^{-1} to lower or higher values indicate the coordination of nitrogen (-NH_2) with metal ions [15]. FT-IR data supported that CEF behaves as tridentate through carboxylate oxygen atom, carbonyl group of β-lactam ring and nitrogen of amine group. The spectrum of Bipy produced peak referred to ν(C=N) group at 1578 cm^{-1} which shifted to lower values in all complexes confirmed Bipy chelated with

two N atoms as bidentate with the metal ions [15,20-23]. The presence of broad band around 3410 cm^{-1} refers to ν(O-H) stretching vibrations, confirming coordinated and/or hydrated H_2O molecules in all complexes [10-15]. The spectra of complexes include a variety of vibrational expressions of new bands with variable intensities, which characterized ν(M-O) and ν(M-N) noticed at 601 and 551 cm^{-1} for (1), at 616 and 515 cm-1 for (2), at 697 and 575 cm-1 for (3), at 651 and 538 cm^{-1} for (4) and at 659 and 524 cm^{-1} for (5). The chelation mode of all complexes was described in Scheme 2.

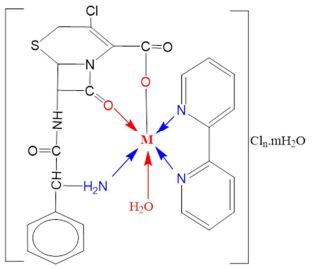

No.	M	n	m
(1)	Cr(III)	2	3
(2)	Co(II)	1	2
(3)	Cu(II)	1	-
(4)	Zn(II)	1	2
(5)	Cd(II)	1	5

Scheme 2: Chelation mode of CEF and Bipy with M

3.3 Ultraviolet-visible spectra and μ_{eff}

UV-vis spectra (Figure S2) and magnetic susceptibility were done and the obtained data were tabulated in Table 3. Electronic spectra of CEF showed one peak at 295 nm assigned to π→π* and two peaks at 320 and 390 nm may be revealed to n→π* transition [11,12]. Also, Bipy gives two peaks at 284 and 347 nm which assigned to transitions [15]. The change of π→π* and n→π* peaks to higher or lower wavelengths and appearance of new peaks for complexes is attributed to chelation of CEF and Bipy. Electronic spectrum of octahedral Cr(III) complex with μeff = 3.70 B.M., 10Dq = 229 $kJmol^{-1}$ and crystal field stabilization energy (CFSE) = -274, showed new peaks at 460 nm attributed to ligand metal charge transfer (LMCT) and d-d transition peak at 521 nm attributed to 4A2g(F)→4T2g(F) transition [13,29]. For Co(II) complex with μeff, 10Dq and CFSE are 1.80 B.M., 237 $kJmol^{-1}$ and -190+2P, respectively, supporting low spin octahedral structure with d-d transition peak found at 505 nm revealed to 4T1g(F) → 4T1g(B) transition [11,15]. For Cu(II) complex, the band at 506 nm revealed to 2B1g→2Eg transition with μeff, 10Dq and CFSE are 1.73 B.M., 236 kJmol-1 and -142+4P, respectively, supporting distorted octahedral geometry [13,30-32]. Also, for complexes of Zn(II) and Cd(II) with μeff = 0 (d10) showed new peaks at 420 and 435 nm supporting to LMCT. 1.0x10-3 M solution of complexes was used, the values of molar absorptivity (ε) for all complexes (Table 3) were calculated using equation: A = εcl, where, A = absorbance, c = $1.0x10^{-3}$ M, l = length of cell (1 cm). We made a chart for a relation between A and ε for ligands and metal complexes (Figure S3).

3.4 Optical band gap energy (E_g)

E_g for compounds were estimated using the absorption bands in UV spectra, which exhibit an abrupt increase in absorption known as the absorption edge. E_g were calculated from Tuac's equation (2) to clarify the conductivity of the compounds [**33**,**34**].

$$\alpha h\nu = \left(E - E_g\right)^n \qquad (2)$$

Where, E = energy of photon, n = ½ and 2 for direct and indirect transitions and α (absorption coefficient) =1/dln(1/T), T = estimated transmittance and d = optical path length of the cuvette.Figure 1 depicts the plotting of $(\alpha h\nu)^2$against E, E_g is obtained by extrapolation of the linear component of the curve to $(\alpha h\nu)^2 = 0$.E_g values = 3.80, 3.60, 3.20, 3.00, 3.10 and 3.00 eV for **CEF**, **(1),** **(2)**, **(3),** **(4)** and **(5)**, respectively. The smaller E_g values of complexes compared with **CEF** may be due to migration of electrons toward metal ions [**35**]. The metal complexes found more electro-conductive by facilitating electronic transitions between LUMO-HOMO energy states and semiconductors which may be thought of as possible solar radiation-capturing materials for solar cell applications according to E_g data [**36**,**37**].

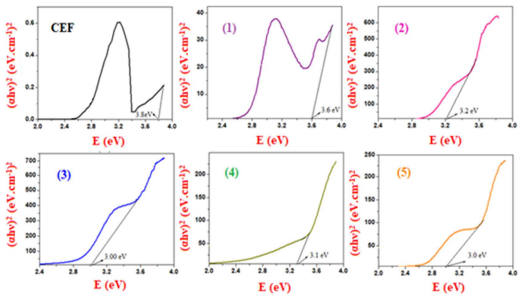

FIGURE 1 Allowed direct band gaps of **CEF** and our complexes

3.5 ^{1}H NMR spectra

^{1}H NMR experimental data of **CEF**, **Bipy,** Zn(II) and Cd(II) compounds were detected (Figure S4) and listed

in Table 4. ^{1}H NMR values of **CEF** δ:11.42 (s, 1H, –COOH), δ:10.90 (s, 2H, –NH_2), δ:7.22-8.47 (m, 5H, –H aromatic), δ:5.82 and 5.94 (d, 2H, β–lactam), δ:3.60 (s, 1H, NHC=O), δ:3.45 (s, 2H, S-CH_2). For **Bipy,** ^{1}H NMR spectrum shows the aromatic ring protons found in the range δ: 7.12-8.79 (m, J = 3.75 Hz, 5H, –H aromatic) **[10,38]**. The disappeared of distinguish signal at δ: 11.42 ppm (-COOH) from the spectra of complexes supporting the coordination of **CEF** with metal ions upon deprotonation **[10]**. The shift of signals for NH_2 δ:10.90 ppm to lower value in spectra for Zn(II) and Cd(II) complexes to 10.30 ppm, confirming coordination of this group to the metal ion. On comparing **CEF** and **Bipy** with their complexes, the signals of aromatic protons were found with some spectra shifts resulting from chelating of **CEF** and **Bipy** with metal ions (Table S1) **[36]**. The recorded values at 4.33 to 4.97 ppm were attributed to H_2O in complexes **[10-15]**.

TABLE 4 ^{1}H NMR values (ppm) and tentative assignments for **CEF, Bipy** and their metal complexes

Compounds	δ (ppm)	
	Experimental	Calculated
CEF	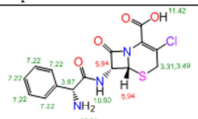	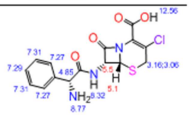
Bipy	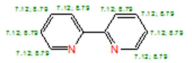	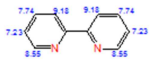
Zn(II) and Cd(II) complexes	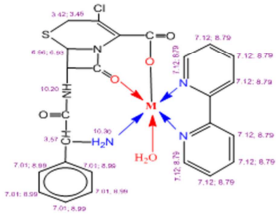	

3.6 X-ray diffraction

XRD of **CEF**, **Bipy** and their complexes were recorded over 2θ from 0 to 60° (Figure 2)and the data listed in Table5. The strong sharp peaks suggested that complexes **(3)**, **(4)** and **(5)** have high crystallinity but complexes **(1)** and **(2)** were amorphous **[20]**. XRD pattern of **CEF**, **Bipy** and their complexesexhibited the highest intensity (100%) at 2θ = 27.11, 16.99, 32.00, 32.67, 27.26, 21.22 and 27.75. The crystallite size (C_s) of the tested compounds was calculated using Debye-Scherer equation (3), C_s of compounds was ranged from 46.49 to 82.06 nm which confirmed nano-size structure.

$$Cs = \frac{k\lambda}{\beta \cos\theta} \qquad (3)$$

Where, C_s is the crystallite size, k is Scherer constant (0.9), λ is the X-ray beam wavelength (0.15405 nm), β is the full width at half maximum (FWHM) of the diffracted peak in (radians), and θ is the diffraction angle. Complexes D values ranged at (1.485–4.627)×10^{-4} nm^{-2} and dislocation line of the complexes (ε) found in the range (10.12 -23.09)×10^{-2} rad.

$$D = \frac{1}{C_s^2} \qquad (4)$$

$$\varepsilon = \frac{\beta}{4\tan\theta} \qquad (5)$$

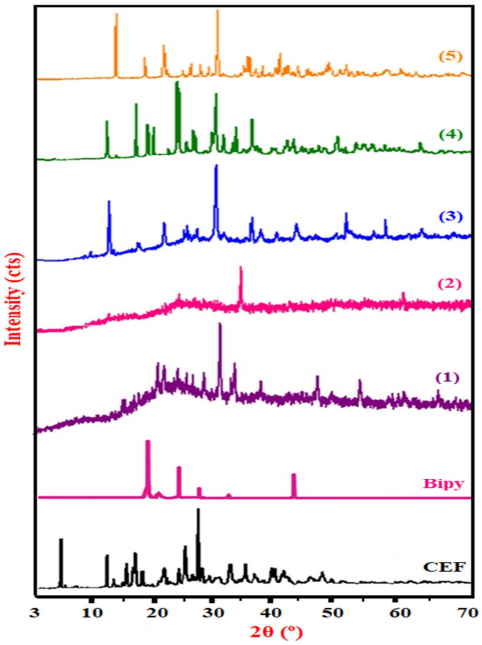

Figure 2: XRD spectra of **CEF**, **Bipy** and their complexes

TABLE 5 C_t of **CEF**, **Bipy**, and complexes calculated from XRD pattern.

Compounds	2θ (°)	d Value (nm)	FWHM	C_t (nm)	D × 10^{-4} (nm^{-2})	ε × 10^{-2} (rad)
CEF	27.11	0.328	0.100	79.97	1.564	10.36
Bipy	16.99	0.522	0.118	68.01	2.162	19.76
(1)	32.00	0.279	0.172	46.62	4.601	14.99
(2)	32.67	0.274	0.155	51.76	3.733	13.22
(3)	27.26	0.327	0.172	46.49	4.627	17.75
(4)	21.22	0.418	0.173	82.06	1.485	23.09
(5)	27.75	0.321	0.100	79.99	1.563	10.12

3.7Thermal studies

Thermogravimetric analyses (TG- DTG- DTA) were done under N_2 flow (Figure S5). Table6 gives the maximum temperature (T_{max}), weight loss %, lost species and final residue. TG of **CEF** indicates that **CEF** decomposed in three steps, the 1st one occurs at 80 °C with weight loss 4.61% (calc. 4.63%) corresponding to loss of NH_3, with exothermic DTA at 78.85 µV. 2nd stage occurs at 206 °C with weight loss 48.03% (calc. 48.02%), corresponding to loss C_2H_2+HSCN+2CO+0.5Cl_2. The 3rd stage found at T_{max} 541 °C, weight loss 40.86% (calc. 48.02%), and loss of $4C_2H_2$+ NO_2. The actual weight loss from these three stages is equal to 93.48%, very closer to calculated value 93.47%, leaving 2C as a residue. Literature survey for thermal decomposition of **Bipy**revealed one degradation stage at 164 °C (weight loss 99.64%, calc. 100%) with E_a 75.70 kJ mol^{-1} [**15**]. TG of **(1)**, **(2), (3), (4)** and **(5)** complexes have three degradation steps, 1st one found at T_{max}(110, 95, 95, 118 and 100 °C), respectively, with weight loss 7.51, 5.34, 2.70, 5.30 and 11.54%, respectively, (calc. 7.52, 5.36, 2.74, 5.32 and 11.56%) corresponding to the loss 3H_2O, 2H_2O, H_2O, 2H_2O and5H_2O, respectively. The 2nd step occurred with T_{max} 240, (181, 232, 345), 218, (161, 219) and (220, 342, 389, 450) °C, respectively, with loss43.52, 52.49, 61.72, 42.40 and 52.13%, respectively, (calc. 43.77, 52.54, 61.74, 42.44 and 52.15%) corresponding to the loss 7C_2H_2+C_2N_2+Cl_2+0.5H_2O, 3C_4H_2+H_2S+2CO_2+0.5Cl_2+N_2+NH_3, 6C_2H_2+Cl_2+3CO+H_2S+N_2O+NH_3,7C_2H_2+C_2N_2+0.5Cl_2 +H_2O,and 6C_2H_2+H_2S+Cl_2+3CO+N_2O+NH_3 supported with DTA at 4.11, 8.05, 4.66, -1.59 and -11.22 µV, respectively. The 3rd step occurred with T_{max} 600, 585, 535, 465 and 581°C, respectively, with weight loss38.25, 29.25, 25.94, 42.55 and 21.82%, respectively, (calc. 38.12, 29.14, 25.86, 42.44 and 21.84%) corresponding to loss 3C_2H_2+3CO+H_2S+1.5N_2+0.5Cl_2, 4C_2H_2+C_2N_2+HCl+1.5H_2, 2C_4H_2+C_2N_2+H_2O, 3C_2H_2+CO+SO_2+C_2N_2+HCl+NO , and 2C_4H_2+C_2N_2+H_2O, respectively, leaving 0.5Cr_2O_3, CoO+C, Cu, Zn, and **C**das a residue in agreement with the theoretical values 10.59, 12.96, 9.66, 9.65 and 14.45%, respectively. The data of CHN and atomic absorption (Table 1) agree well with the found metal content from the residual weight. Infrared spectra of the final residues disclosed the lack of all peaks criterion of chelated of **CEF** and **Bipy**, also characteristic peaks of metal oxides were appeared for complexes **(1)** and **(2)**

TABLE 6 T_{max} (°C) and weight loss values of decomposition stages for **CEF, Bipy** and their metal complexes.

Compounds	Decomposition steps	T_{max} (°C)	Weight Loss (%) Calc.	Found	Lost Species
	1st	80	4.63	4.61	NH_3
CEF	2nd	206	48.02	48.03	C_2H_2+HSCN+2CO+0.5Cl_2
	3rd	541	40.82	40.86	4C_2H_2+ NO_2
	Total loss		93.47	93.48	
	Residue		6.53	6.50	2C
	1st	164	100	99.64	4C_2H_2 + C_2N_2
Bipy	Total loss		100	99.64	
	1st	110	7.52	7.51	3H_2O
	2nd	240	43.77	43.52	7C_2H_2+C_2N_2+Cl_2+0.5H_2O
(1)	3rd	600	38.12	38.25	3C_2H_2+3CO+H_2S+1.5N_2+0.5Cl_2
	Total loss		89.41	89.28	
	Residue		10.59	10.72	0.5Cr_2O_3
	1st	95	5.36	5.34	2H_2O
	2nd	181,232,345	52.54	52.49	3C_4H_2+H_2S+2CO_2 +0.5Cl_2+N_2+NH_3
(2)	3rd	585	29.14	29.25	4C_2H_2 + C_2N_2+HCl+1.5H_2
	Total loss		87.04	87.08	
	Residue		12.96	12.92	CoO+C
	1st	95	2.74	2.70	H_2O
	2nd	218	61.74	61.72	6C_2H_2+Cl_2+3CO+H_2S+N_2O+NH_3
(3)	3rd	535	25.86	25.94	2C_2H_2 +C_2N_2+H_2O
	Total loss		90.34	90.36	
	Residue		9.66	9.64	Cu
	1st	118	5.32	5.30	2H_2O
	2nd	161,219	42.44	42.40	7C_2H_2+C_2N_2+0.5Cl_2+H_2O
(4)	3rd	465	42.59	42.55	3C_2H_2+CO+SO_2+C_2N_2+HCl+NO
	Total loss		90.35	90.25	
	Residue		9.65	9.75	Zn
	1st	100	11.56	11.54	5H_2O
	2nd	220,342,389,450	52.15	52.13	6C_2H_2+H_2S+Cl_2+3CO,N_2O+NH_3
(5)	3rd	581	21.84	21.82	2C_2H_2 + C_2N_2+H_2O
	Total loss		85.55	85.49	
	Residue		14.45	14.51	Cd

3.8 Computational details

Equilibrium geometrical structures of **CEF** and synthesized complexes were investigated by DFT calculations using GAUSSIAN 98W package of the programs [**39**], with B3LYP/CEP-31G level of theory [**40**] basis set was applied for the all calculations. The accumulated atomic charges were computed using the natural atomic orbital populations. The high basis set was chosen for detection of the energies and different parameters at a highly accurate level.

3.8.1 Geometrical structure of CEF

The obtained equilibrium geometrical parameters, total energy, dipole moment, bond lengths, bond angles and dihedral angles of **CEF** were given in Table S1 confirmed that, **CEF** is non-linear completely but it divided into two parts in two different planes around C12-N14 bond (Figure 3). The dihedral angle N4C3C8O10, equal 2.75° ≈ 0.0°, so O10 of carboxylate group is lying in the same side occupied by N10 of the amide group. Also, the value of dihedral angle C3N7C11O13 is -9.03° ≈ 0.0°, this result indicates that O13 of β-lactam group, can participate in chelation with metal ion after small rotation around N4-C11 by angle 9.03° to be laying in the same plane of O10 of carboxylic group. Also, the value of dihedral angle O13C11C12N14 (-62.05°), confirms the chelation of O13 after rotation with small angle around N4-C11. In contrast to the location, O17 of the amide group which laying out the plane occupied by other donating sites, with dihedral angle

C12N14C15O17 and C2318C15O17 are 178.31° and -113.35°. The results confirm the participating of O17 in chelation with metal ion is more difficult which required higher energy and greater angle to rotate and found in the plane of coordinated atoms, so **CEF** favors chelation with metal ion through O13 not through O17. According to dihedral angle N14C15C18N20 (-63.51°), N20 can participate in chelation with metal ion after rotation with small angle to be lying in the same plane of other donating sites.

The ligand molecule exhibits significant steric effects, leading to the easy rotation of different fragments around the existing single bonds [**41**]. Based on the obtained results, the reaction rate of **CEF** with the metal ion is relatively slow, requiring additional time for the chelation process. The optimized geometry of **CEF** reveals calculated dihedral angle that is consistent with the UV spectra of similar compounds [**42**]. The UV spectrum exhibits two notable characteristics: (i) the presence of n→π* transitions associated with the presence of non-bonding electrons, and (ii) the maximum absorption bands are observed in the UV region. These results indicate the degree of planarity of the molecule, and the computed data presented in Table S1 align with those derived from X-ray data [**43**]. The charge distribution on **CEF**, with dipole moment (μ) and total energy (E) were 6.434 D and -145698.064 k cal/mol, suggests the more stability of **CEF**. Additionally, the absence of both net positive and negative charged poles on the molecule supporting the non-planarity of **CEF**.

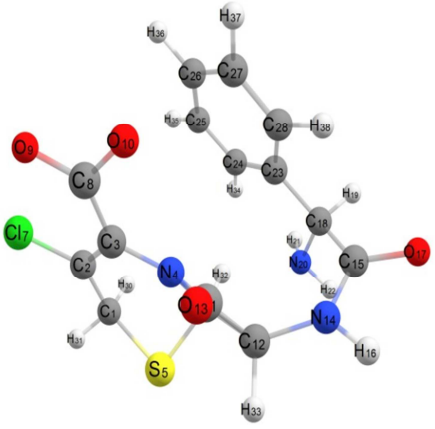

Figure 3: The optimized geometrical structure of **CEF** by using DFT calculations

3.8.2 Geometrical structure of complexes

The objective of this study was to determine the optimized equilibrium geometry of the prepared complexes and analyze their UV-vis spectra using DFT calculations. There are different equilibrium geometrical parameters as, bond lengths, bond angles and dihedral angles, in addition to total energy, E and dipole moment, μ of the complexes were listed in Table S2.The optimized geometrical structures of all studied complexes considered as distorted octahedral structures (Figures S6-S10) where, the central metal ions, Cr(III), Co(II), Cu(II), Zn(II) and Cd(II) in complexes is binding with **CEF** via O6, O1, N12 and **Bipy** through N13 and N16 and complete the coordination sphere with O17 of water molecule. Bond length M-N13 was varied between 1.870 and 2.468 Å, while M-N16 varied between 1.871 and 2.465 Å [**44-46**]. The bond lengths M-O1, M-O6 and M-N12 of **CEF** found from 1.958 to 2.339, 2.011 to 2.497 and 1.918 to 2.309 Å, respectively [**47-51**]. In addition, the bond length M-O17 changed from 1.843 and 2.258 Å [**52-54**]. According to the values of the obtained angles around the metal ions with bonded donating atoms (Table S2),**CEF** and **Bipy** molecules not laying in the same plane but they are perpendicular to each other. Also, H_2O molecule in trans-form with respect to O1 of carboxylate group for **CEF** in some complexes or in cis form with N13 and N16 of **Bipy**molecule forming distorted octahedral structure.

3.8.3 Charge distribution analysis

The charge distribution analysis of **CEF** and complexes was conducted using natural population analysis (NPA), and significant data were listed in Table S3. The charge distribution on the coordinated atoms of **CEF**, indicates the absence of net negative and positive poles, resulting from weak μ (6.434 D). The charge density data (Table S3) showed that Cr(III) complex has highly charge density accumulated (0.381). In contrast, the other complexes exhibit lower charge densities, with the smallest charge being observed on Cu(II) complex (0.160), and a negative charge (-0.063) on Co(II) ion. The negative charge is distributed across all atoms, with a significant percentage concentrated on O and N atoms of **CEF** and **Bipy**, on other hands, the atoms carry positive charges in all complexes. According to accumulated charges on all atoms for Cr(III) and Cd(II) complexes indicate an electron back-donation from metal ions to π* orbitals of **CEF** and **Bipy**. This conclusion is

further supported by comparing the calculated charge density values on the different donating sites (N and O) of **Bipy** and **CEF** in the complexes. The direction of μ vector in the complexes which depends on the centers of negative and positive charges was determined from the distribution of atomic charges over all donating atoms.

3.8.4 Frontier molecular orbitals (MOs)

MOs play a significant role in the electrical and UV-vis characteristics [**55**]. An electronic system with smaller energy gap (ΔE) between the lowest unoccupied molecular orbital (LUMO) and the highest occupied molecular orbital (HOMO) is generally more reactive compared to a system with larger ΔE [**56**]. ΔE value is closely associated with the reactivity and stability of the molecule. A smaller ΔE value suggests lower kinetic stability and slightly higher chemical reactivity. It is worth noting that adjacent orbitals are often closely spaced in the frontier region. ΔE values of studied compounds varied, with Cr(III) complex exhibiting ΔE 0.045 eV, indicating higher reactivity, and Zn(II) complex with lower ΔE (0.090 eV), is low reactive than **CEF** (ΔE = 0.122 eV). Consequently, there is easier electronic movement between HOMO and LUMO orbitals, leading to significant peak around 290 nm in UV-vis spectra of all complexes.

The nodal properties of MOs in all complexes (Figure S11) provide evidence of strong orbital overlap, orbital delocalization, and low number of nodal planes. These characteristics, along with the nodal properties, contribute to UV-vis spectra, which are characterized by high-intensity bands with lower energy and the presence of charge transfer transitions. The various MOs exhibit different degrees of localization on different fragments of the complexes, and this rationalization holds true for molecular orbital analysis of all investigated complexes. ΔE values for all complexes as determined from theoretical calculations (Table S3) have lower values compared with free **CEF** indicating that the complexes more reactive than **CEF**. Figure S10 illustrates the iso-density surface plots of HOMO and LUMO for **CEF** and its complexes. The electron density of LUMO and HOMO is delocalized over all atoms and spreads across all fragments of **CEF** molecule. The hardness, η = (I-A)/2, where I is ionization energy, A is electron affinity, and (I-A) is equal to ΔE for **CEF** and its complexes were calculated. All complexes with smaller ΔE and η values ranging from 0.045 for Zn(II) complex to 0.0225 for Cr(III) complex considered as soft and stable compounds with easily electronic transition inside them compared with **CEF** [**57**]. Several quantum chemical parameters, global softness (S), electronegativity (χ), absolute softness (σ), chemical potential (Pi), global electrophilicity (ω), and additional electronic charge (ΔN_{max}), were calculated based on energy of LUMO and HOMO for **CEF** and complexes. The data assigned Cr(III) complex as soft one (σ = 44.444 eV) and Zn(II) complex as hard (σ = 22.222 eV).

3.8.5Excited state

Electronic transitions for **CEF** and complexes described as n→π*, π→π*, LMCT and d-d transitions. Energies of LUMO and HOMO for **CEF** and its complexes were listed in Table S4. HOMO state assigned as electron donor and LUMO state electron acceptor in the reaction profile. Electron density of HOMO for Co(II), Cd(II), and Zn(II) complexes is primarily localized on **CEF**, with percentages 87.2%, 100%, and 70.6%, respectively but for Cr(III) complex, the electron density localized on the atoms of **Bipy** only with 83.7%, while Cu(II) complex, electron density delocalized and spreads over all atoms with different percentages. In LUMO state, the electron density is localized only on all atoms of **Bipy** for Zn(II) and Cd(II) complexes, with percentages of 100% and 98.6%. Also, the electron density is delocalized over all atoms of Cr(III), Co(II), and Cu(II) complexes, , indicating mixed n→π* and π→π* transitions. The noteworthy feature of the studied complexes is that LUMO orbitals primarily focus on donating atoms (O and N) and M. For Cr(III) and Co(II) complexes, LUMO orbital is localized and spreads over all donating atoms with for 66.4% and 74.4%, these values enhance M→π* of ligands.

3.9 Bactericidal and fungicidal efficiencies

Disc diffusion method was used to evaluate the antimicrobial effectiveness of **CEF**, **Bipy**, and complexes against pathogenic bacteria and fungi [**24**,**25**]. The analysis of antibacterial activity for all compounds is presented in Table 7 and Figures S12,13. The data indicating that Gentamicin, Ampicillin, and Nystatin compounds were not effective against the tested microorganisms.Cu(II) complex showed very highly significant activity against *E. coli* and highly significant activity against the other bacterial species. Complex **(4)** demonstrated highly significant activity against *S. aureus*, *S. mutans*, and *E. coli* highly and significant activity against *K. pneumonia*. Complex **(1)** displayed significant activity against *S. mutans*, *E. coli*, and *K. pneumonia*, and highly significant activity against *S. aureus*. On the other hand, complex **(5)** exhibited significant activity against *S. aureus*, *S. mutans*, and *K. pneumonia*, and

highly significant activity against *E. coli*. The data supporting that all complexes exhibited greater activity compared to the free ligands. The effectiveness of complexes can be attributed to their ability to easily penetrate cells due to cell permeability and the presence of a lipid membrane surrounding the cells. This characteristic is of significant importance for the complexes [**46,58,59**]. Moreover, the antibacterial effects of the complexes may involve one or more of the following mechanisms: i) causing damage to the cell wall, ii) inhibiting plasma membrane functions such as permeability and energy generation, iii) disrupting protein synthesis, iv) inhibiting nucleic acid (DNA or RNA) activity, v) impeding enzyme function, and vi) acting as antimetabolites. The activity order of the complexes against bacterial strains was **(2)> (3) >(4)>(1)** ≈ **(5)**. Complex **(1)** exhibited highly significant activity against *C. albicans* and significant activity against *A. nigar*, while complex **(5)** displayed significant activity against *A. nigar* compared to the reference control. Complexes **(2)**, **(3)**, and **(4)** did not show detectable activity against the two fungal species. The practical data listed in Table 8 indicated that, the order of the inhibition zone of $[Co(CEF)(Bipy)(H_2O)]Cl.2H_2O$ and $Cu(CEF)(Bipy)(H_2O)]Cl.H_2O$ is more active than the other previous complexesin case of in all tested bacteria.

TABLE 7 Antimicrobial properties of **CEF**, **Bipy** and their complexes.

Compounds	Tested G+ve and G-ve Bacterial Strains											
	S. aureus			*S. mutans*			*E. coli*			*K. pneumonia*		
	D.iz[a] (mm)	AI[b] (%)	MIC[c] (µg/mL)	D.iz (mm)	AI (%)	MIC (µg/mL)	D.iz (mm)	AI (%)	MIC (µg/mL)	D.iz (mm)	AI (%)	MIC (µg/mL)
CEF	10.3±0.6	51.50	0.050	9.3±0.6	33.57	0.075	8.7±0.6	31.86	0.025	9.3±1.0	37.20	0.050
Bipy	8.7±0.6	43.50	0.025	7.3±0.6	26.35	0.050	14±0.6	51.28	0.050	7.3±0.6	29.20	0.025
(1)	20.0^{ns}±1.0	100.00	0.075	14.7^{ns}±0.6	53.06	0.025	15.0^{ns}±1.0	54.94	0.050	16.0^{ns}±1.0	64.00	0.050
(2)	26.7^{ns}±0.6	133.50	0.100	30.3^{ns}±0.6	109.38	0.100	32.7^{ns}±0.6	119.78	0.100	30.3^{ns}±0.6	121.20	0.100
(3)	25.7^{ns}±0.6	128.50	0.075	25.3^{ns}±0.6	91.33	0.100	27.3^{ns}±0.6	100.00	0.100	26.0^{ns}±1.0	104.00	0.075
(4)	21.3^{ns}±0.6	106.50	0.050	20.7^{ns}±0.6	74.72	0.075	24.0^{ns}±1.0	87.91	0.075	22.7^{ns}±0.6	90.80	0.025
(5)	16.3^{ns}±0.6	81.50	0.050	18.7^{ns}±0.6	67.50	0.025	18.0^{ns}±1.0	65.93	0.100	18.7^{ns}±0.6	74.80	0.050
Standards Gentamicin	----	----	----	----	----	----	----	27.3±0.6	100.00	0.025	25.0±1.0	100.00	0.025
Ampicillin	20.0±1.0	100.00	----	27.7±0.6	100.00	----	----	----	----	----	----	----	----

Compounds	Tested Fungal Strains					
	C. albicans			*A. nigar*		
	D.iz (mm)	AI (%)	MIC (µg/mL)	D.iz (mm)	AI (%)	MIC (µg/mL)
CEF	9.0±1.0	42.85	0.025	ND	----	----
Bipy	28.0±1.0	133.33	0.075	13.0±1.0	67.35	0.050
(1)	21.0^{ns}±1.0	100.00	0.100	12.0^{ns}±0.6	62.17	0.075
(2)	ND	----	----	ND	----	----
(3)	ND	----	----	ND	----	----
(4)	ND	----	----	ND	----	----
(5)	11.7^{ns}±0.07	55.71	0.025	13.0^{ns}±1.0	67.35	0.050
Standards Nystatin	21.0±1.0	100.00	----	19.3±0.6	100.00	----

Statistical significance: P^{ns}; P not significant, $p > 0.05$; P^{*1}; P significant, $p < 0.05$; P^{*2}; P highly significant, $p < 0.01$; P^{*3}; P very highly significant, $p < 0.001$; student's *t*-test (paired). [a] D.iz: diameter of inhibition zone (mm); [b] AI: activity index (%); [c] MIC: minimum inhibitory concentration (µg/mL); ND: not detectable.

4. Conclusion

Some spectroscopic techniques, thermal investigations and DFT were used to prove the molecular structures of Cr(III), Co(II), Cu(II), Zn(II) and Cd(II) complexes with mixed ligands **CEF** and **Bipy**. The data confirmed that, **CEF** chelated with the metal ions as tridentate ligand through nitrogen of amine group and two oxygen atoms of carbonyl groups of lactam ring and caroboxylate group. While, **Bipy** reacted through two nitrogen atoms forming distorted octahedral complexes. The molar conductance values of complexes indicated that all complexes were electrolyte with 1:2 for Cr(III) and 1:1 for other complexes. The results of DFT calculations show that the computed geometrical parameters coincide quite well with an experimental data. Cr(III) complex with smaller ΔE value (0.045 eV) is more reactive than all other complexes while, Zn(II) complex with higher ΔE value (0.090 eV) is less reactive. According to antibacterial activity data, Co(II) complex had strong activity against tested G+ve and G-ve bacterial strains compared to other complexes. Also, Cr(III) complex showed highly significant and significant against two fungi tested species.

Acknowledgements

The authors submit their acknowledgment to their University (Zagazig, Egypt) for encouragement the team work to do this work.

Declarations

Conflict of interest: All authors declare that, there is no competing of interests

References

[1] Derya T, Burcu DT, Mustafa D, Aysegul G, Sibel AO. Synthesis, Characterization, Biological Activity and Voltammetric Behavior and Determination of Cefaclor Metal Complexes. Current AnalyChem 2010; 6:316-328.

[2] United States Pharmacopoeia XXIII, United States pharmacopoeia convection, Rockville, MD, 1993.

[3] Božić B, Korać J, Stanković DM, Stanić M, Romanović M, Pristov JB, Spasić S, Bijelić AP, Spasojević, Bajčetić M. Coordination and redox interactions of β-lactam antibiotics with Cu^{2+} in physiological settings and the impact on antibacterial activity. Free Radical Biology and Medicine 2018;129:279–285. https://doi.org/10.1016/j.freeradbiomed.2018.09.038.

[4] Agarwal P, Asija S, Deswal Y, Kumar N. Recent advancements in the anticancer potentials of first row transition metal complexes. J. of the Indian chem. Soc 2022;99:100556. https://doi.org/10.1016/j.jics.2022.100556.

[5] Deswal Y, Asija S, Tufail A, Dubey A, Deswal L, Kumar N, Saroya S, Kirar JS, Gupta NM. Instigating the in vitro antidiabetic activity of new

tridentate Schiff base ligand appended M(II) complexes: From synthesis, structural characterization, quantum computational calculations to molecular docking, and molecular dynamics simulation studies. Appl. Organomet. Chem 2023;37: e7050.
https://doi.org/10.1002/aoc.7050.
[6] Deswal Y, Asija S, Dubey A, Deswal L, Kumar D, Jindal DK, Devi J. Cobalt(II), nickel(II), copper(II) and zinc(II) complexes of thiadiazole based Schiff base ligands: Synthesis, structural characterization, DFT, antidiabetic and molecular docking studies. J. Mol. Struct 2022;1253:132266.
https://doi.org/10.1016/j.molstruc.2021.132266.
[7] Lowe J, da-Silva RT, Souza EH. Dissecting copper homeostasis in diabetes mellitus. IUBMB Life 2017; 69: 255–262.
https://doi.org/10.1002/iub.1614.
[8] Poole K. At the Nexus of Antibiotics and Metals: The Impact of Cu and Zn on Antibiotic Activity and Resistance. Trends Microbiol 2017; 25:820–832.
https://doi.org/10.1016/j.tim.2017.04.010.
[9] Deswal Y, Asija S, Tufail A, Dubey A, Deswal L, Kumar N, Kirar JS, Gupta NM, Barwa P. Metal Complexes of 1,2,4-Triazole Based Ligand: Synthesis, Structural Elucidation, DFT Calculations, Alpha-Amylase and Alpha-Glucosidase Inhibitory Activity Along with Molecular Docking Studies. Journal of Inorganic and Organometallic Polymers and Materials 2024;34:144-160.
https://doi.org/10.1007/s10904-023-02808-4.
[10] Abbass LM, Sadeek SA, El-Raouf Aziz MA, Zordok WA, El-Attar MA. Synthesis of some new nanoparticles mixed metal complexes of febuxostat in presence of 2,2'-bipyridine: Characterization, DFT, antioxidant and molecular docking activities. J. Mol. Liq 2023;386:122460.
https://doi.org/10.1016/j.molliq.2023.122460.
[11] Abd El-Hamid SM, Sadeek SA, Mohammed SF, Ahmed FM, El-Gedamy MS. N_2O_2-chelate metal complexes with Schiff base ligand:Synthesis, characterisation and contribution as apromising antiviral agent against human cytomegalovirus. Appl. Organomet. Chem 2023;37:e6958.
https://doi.org/10.1002/aoc.6958.
[12] Abd El-Hamid SM, Sadeek SA, Mohammed SF, Ahmed FM, El-Gedamy MS. Newly synthesised Schiff base metal complexes, characterisation, and contribution as enhancers of colon cancer cell apoptosis by overexpression of P53 protein. Appl. Organomet. Chem 2023;37:e7129.
https://doi.org/10.1002/aoc.7129.
[13] El-Attar MS, El-Sayed HA, Sadeek SA, Zordok WA, Kamal HM. Characterization, DFT calculations and antimicrobial assays of some novel nanoparticles mixed ligand complexes of 5-cyano-6-phenyl-2-thiouracil in presence of 1,10-phenanthroline. J. Mol. Liq 2023;384:122149.
https://doi.org/10.1016/j.molliq.2023.122149**.**
[14] El-Attar MS, Sadeek SA, El-Sayed HA, Kamal HM, Elshafie HS. Structural and antimicrobial investigation of some new nano-particles mixed ligands metal complexes of Ethyl 6-amino-4-(4-chlorophenyl)-5-cyano-2-methyl-4H-pyran-3-carboxylate in presence of 1,10-phenanthroline. Inorganics 2023;11:220(1-17).
https://doi.org/10.3390/inorganics11050220**.**
[15] Kamal HM, El-Sayed HA, SadeekSA ,Zordok WA, El-Attar MS. Spectroscopic characterization, DFT modeling and antimicrobial studies of some novel nanoparticles mixed ligand complexes of NS bidentate ligand in presence of 2,2'-bipyridine. J. Mol. Liq 2023; 376:121404.
https://doi.org/10.1016/j.molliq.2023.121404.
[16] Chohan ZH. Synthesis of cobalt(II) and nickel(II) complexes of Ceclor (cefaclor) and preliminary experiments on their antibacterial character. Chem. pharm. Bull 1991; 39: 1578-1580.
https://doi.org/10.1248/cpb.39.1578.
[17] El-Ghamry HA, Alharbi BK, Takroni KM, Khedr AM. A series of nanosizedCu(II) complexes based on sulfonamideazo dye ligands: An insight into complexes molecular structures, antimicrobial, antitumor and catalytic performance for oxidative dimerization of 2-aminophenol. Appl. Organomet. Chem 2023;37: e6978.
https://doi.org/10.1002/aoc.6978.
[18] El-Ghamry HA, Takroni KM, AL-Rashidi DO, Alfear ES, Alsaedi RA. Design, spectral, thermal decomposition, antimicrobial, docking simulation and DNA binding tendency of sulfisoxazoleazo dye derivative and its metal chelates with Mn^{2+}, Fe^{3+}, Co^{2+}, Ni^{2+}, Cu^{2+}, Zn^{2+} and Cd^{2+}. Appl. Organomet. Chem 2022;36: e6813.
https://doi.org/10.1002/aoc.6813.
[19] Deswal Y, Asija S, Kumar D, Jindal DK, Chandan G, Panwar V, Saroya S, Kumar N. Transition metal complexes of triazole-based bioactive ligands: synthesis, spectral characterization, antimicrobial, anticancer and molecular docking studies. Research on Chemical Intermediates 2022;48:703-729.
https://doi.org/10.1007/s11164-021-04621-5.
[20] Salem AE, Mohammed SF, Sadeek SA, Zordok WA, El-Attar MS. Synthesis, structural elucidation, molecular modeling, and antimicrobial studies of some nanoparticles mixed ligands complexes of cetirizine in presence of 2,20-bipyridine. Appl. Organomet. Chem 2022; 36.
https://doi:10.1002/aoc.6715.
[21] Abd El-Hamid SM, Sadeek SA, Zordok WA, El-Shwiniy WH. Synthesis, spectroscopic studies, DFT calculations, cytotoxicity and antimicrobial activity of some metal complexes with ofloxacin and 2,2′-bipyridine. J. Mol. Struct 2019;1176:422-433.
https://doi.org/10.1016/j.molstruc.2018.08.082.
[22] Fadl AM, Sadeek SA, Magdy L, Abdou MI, El-Shiwiniy WH. Multi-functional epoxy composite coating incorporating mixed Cu(II) and Zr(IV) complexes of metformin and 2,2\-bipyridine as intensive network cross-linkers exhibiting anti-corrosion, self-healing and chemical-resistance performances for steel petroleum platforms. Arab. J. Chem 2021; 14:103367.
https://doi.org/10.1016/J.ARABJC.2021.103367.
[23] El Awady MA, Khalil MMH, Mohamed GG, Salem ANM. Tinuvin-P Metal Complexes as New Photo-Stabilizers for PVC: Synthesis, Characterization and DFT Studies. Egy. J. Chem.

2024;67:127-139.https://doi.org/10.21608/EJCHEM.2024.250821.8921
https://doi.org/10.1016/j.jmrt.2021.09.034.
[24] Khedr AM, El-Ghamry HA, Wahdan KM, Mandour HSA. Synthesis, characterization, antimicrobial, molecular docking simulation, and antitumor assays of nanometric complexes based on new thiazole Schiff base derivative. Appl. Organomet. Chem 2024;38: e7362.
https://doi.org/10.1002/aoc.7362.
[25] Beecher DJ, Wong AC. Identification of hemolysin BL-producing Bacillus cereus isolates by adiscontinuoushemolytic pattern in blood agar. Appl. Environ. Microbial 1994;60:1646-1651. https://doi.org/10.1128/aem.60.5.1646-1651.1994.
[26] Fallik E, Klein J, Grinberg S, Lomaniee CE, Lurie S, Lalazar A, Econ J. Entomol**1993**; 77: 985.
[27] Mohamed AA, Sadeek SA. Ligational and biological studies of Fe(III), Co(II), Ni(II), Cu(II), and Zr(IV) complexes with carbamazepine as antiepileptic drug, Appl. Organomet. Appl. Organomet. Chem 2021;35:e6178.
https://doi.org/10.1002/aoc.6178.
[28] Geary WJ. The use of conductivity measurements in organic solvents for the characterisation of coordination compounds. J. Coord. Chem. Rev 1971;7: 81-122.
https://doi.org/10.1016/S0010-8545(00)80009-0.
[29] Abo baker LO, Mahmoud WH, Taha A, El-Sherif AA. Synthesis, Characterization, Biological and Anticancer Activities Studies of Ternary CephardinePd (II) Complexes. Egy. J. Chem. 2024;67:639-648.https://doi.org/10.21608/EJCHEM.2024.252582.8938.
[30] Khedr AM, Mandour HAS,Wahdan KM, El-Ghamry HA. New nanometric metal complexes based on thiazole derivative as potential antitumor and antimicrobial agents: Full structural elucidation, docking simulation and biological activity studies. J. Mol. Liq 2024; 401:124665.
https://doi.org/10.1016/j.molliq.2024.124665.
[31] El-Saied FA, Salem TA, Metwaly AN, El-Aarag B. Synthesis, characterization and anticancer potency of novel Mn(II), Co(II), and Cu(II) complexes based on N-[(1E)-1-(4-hydroxy-6-methyl-2-oxo-2H-pyran-3-yl)ethylidene]-2-(4-methylanilino)acetohydrazide. Egy. J. Chem. 2024;67:37-55.https://doi.org/10.21608/EJCHEM.2023.196938.7652.
[32] Psomas G, Raptopoulou CP, Iordanidis L, Dendrinou-Samara C, Tangoulis V, Kessissoglou DP. Structurally diverse copper(II)-carboxylato complexes: neutral and ionic mononuclear structures and a novel binuclear structure. Inorg.Chem 2000;39:3024-3028.
https://doi.org/10.1021/ic991476q.
[33] Rashad MM, Hassan AM, Nassar AM, Ibrahim NM, Mourtada A. A new nano-structured Ni(II) Schiff base complex: synthesis, characterization, optical band gaps, and biological activity. Appl. Phys. 2014;117: 877-890.
[34] Tauc J. Optical properties and electronic structure of amorphous Ge and Si. Mat. Res. Bull 1968;3:37- 46.
https://doi.org/10.1016/0025-5408(68)90023-8.
[35] Karipcin F, Dede B, Caglar Y, Hur D, Ilican S, Caglar M, Sahin Y. A new dioxime ligand and its trinuclearcopper(II) complex: Synthesis, characterization and optical properties. Opt. Commun 2007;272:131-137.
https://doi.org/10.1016/j.optcom.2006.10.079.
[36] Sengupta SK, Pandey OP, Srivastava BK, Sharma VK. Synthesis, structural and biochemical aspects of titanocene and zirconocene chelates of acetylferrocenylthiosemicarbazones.Transit.Met.Chem 1998;23:349-353.
[37] Turan N, Gündüz B, Körkoca H, Adigüzel R, Çolak N, Buldurun K. Study of Structure and Spectral Characteristics of the Zinc(II) and Copper(II) Complexes With 5,5-Dimethyl-2-(2-(3-nitrophenyl) hydrazono)cyclohexane-1,3-dione and Their Effects on Optical Properties and the Developing of the Energy Band Gap and Investigation of Antibacterial Activity. J. Mex. Chem. Soc 2014;58:65-75.
[38] Lehmann U, Lach J, Loose C, Hahn T, Kersting B, Kortus J. Binuclear nickel complexes with an edge sharing bis(square-pyramidal) N3Ni(μ-S2)NiN3 core: synthesis, characterization, crystal structure and magnetic properties. Dalton Trans. 2013;42:987-996.
https://doi.org/10.1039/C2DT31973J.
[39] Gaussian 98, Revision A.6, M. J. Frisch, G. W. Trucks, H. B. Schlegel, G. E. Scuseria, M.A.Robb, J.R.Cheeseman, V.G. Zakrzewski, J.A. Montgomery, Jr.,R.E.Stratmann, J.C.Burant, S.Dapprich, J.M.Millam, A.D.Daniels, K.N. Kudin, M.C. Strain, O. Farkas, J. Tomasi, V. Barone, M. Cossi, R. Cammi, B.Mennucci, C. Pomelli, C. Adamo, S.Clifford, J. Ochterski, G. A. Petersson, P. Y. Ayala, Q. Cui, K. Morokuma, D. K.Malick, A.D.Rabuck, K. Raghavachari, J.B. Foresman, J.Cioslowski, J.V.Ortiz, B.B.Stefanov, G.Liu, A.Liashenko, P.Piskorz, I. Komaromi, R.Gomperts,R. L. Martin, D. J. Fox, T. Keith, M. A. Al-Laham, C. Y. Peng, A. Nanayakkara, C. Gonzalez, M. Challacombe, P. M. W. Gill, B. Johnson, W. Chen, M. W. Wong, J. L.Andres, C. Gonzalez, M. Head-Gordon, E. S. Replogle, and J. A. Pople, Gaussian, Inc., Pittsburgh PA, **1998.**
[40] Stevens WJ, Krauss M, Bosch H, Jasien PG. Relativistic Compact Effective Potentials and Efficient, Shared-Exponent Basis Sets for the Third-, Fourth-, and Fifth-Row Atoms. Can. J. Chem 1992;70:612-630.
https://doi.org/10.1139/v92-085.
[41] Abu-EittahRH, Zordok WA. A molecular orbital treatment of piroxicam and its M^{2+}-complexes: The change of the drug configuration in a time of bond formation. J.Mol. Structure: THEOCHEM 2010; 951:14-20.
https://doi.org/10.1016/j.theochem.2010.03.034.
[42] Defazio S, Cini R. Synthesis, X-ray structure and molecular modelling analysis of cobalt(II), nickel(II), zinc(II) and cadmium(II) complexes of the widely used anti-inflammatory

drug meloxicam. J. Chem. Soc. Dalton Trans 2002;22:1888-1897.
https://doi.org/10.1039/B107594M.
[43] Cini R, Tamasi G, Defazio S, Hursthouse MB. Unusual coordinating behavior by three non-steroidal anti-inflammatory drugs from the oxicam family towards copper(II). Synthesis, X-ray structure for copper(II)-isoxicam, -meloxicam and -cinnoxicam-derivative complexes, and cytotoxic activity for a copper(II)-piroxicam complex. J. Inorg. Biochem 2007;101:1140-1152.
https://doi.org/10.1016/j.jinorgbio.2007.04.015.
[44] Altürk S, Avcı D, Bas A¸ o_glu, Tamer €O, Atalay Y, Dege N. Copper(II) complex with 6-methylpyridine-2-carboxyclic acid: experimental and computational study on the XRD, FT-IR and UVeVis spectra, refractive index, band gap and NLO parameters, Spectrochim. Acta. Mol. Biomol. Spectrosc2018 ;190:220-230.
https://doi:10.1016/j.saa.2017.09.041.
[45] Freedman DE, Harman WH, Harris TD, Long GJ, Chang CJ, Long JR. Slow Magnetic Relaxation in a High-Spin Iron(II) Complex. J. Am. Chem. Soc 2010;132:1224-1225.
https://doi.org/10.1021/ja909560d.
[46] Anderson RA, Cheng N, Bryden NA, PolanskyMM, Cheng N, Chi J, Feng J. Elevated intakes of supplemental chromium improve glucose and insulin variables in individuals with type 2 diabetes. Diabetes 1997;46: 1786-1791.
https://doi.org/10.2337/diab.46.11.1786.
[47] Kovalchukova OV, Ryabov MA, Dorovatovskii PV, Zubavichus YV, Utenyshev AN, Kuznetsov DN, Volyansky OV, Voronkova VK, Khrustalev VN. Synthesis and characterization of a series of novel metal complexes of N-heterocyclic azo-colorants derived from 4-azo-pyrazol-5-one. Polyhedron 2017;121:41-52.
https://doi.org/10.1016/j.poly.2016.09.047.
[48] Gangu KK, Maddila S, Mukkamala SB, Jonnalagadda SB. Synthesis, characterisation and catalytic activity of 4, 5-imidazoledicarboxylate ligated Co(II) and Cd(II) metal-organic coordination complexes. J. Mol. Struct 2017;1143: 153-162.
https://doi.org/10.1016/j.molstruc.2017.04.083.
[49] Yue YF, Sun W, Gao EQ, Fang CJ, Xu S, Yan CH. Syntheses and crystal structures of three Mn(II) complexes with 2-hydroxynicotinate. Inorganica.Chimica.Acta 2007;360:1466-1473.
https://doi.org/10.1016/j.ica.2006.08.014.
[50] De Oliveira EH, Medeiros GEA, Peppe C, Brown MA, Tuck DG. The direct electrochemical synthesis of some metal derivatives of lapachol. Can. J. Chem 1997;75:499-506.
https://doi.org/10.1139/v97-058.
[51] Repich HH, Orysyk SI, Orysyk VV, Zborovskii YL, Melnyk AK, Trachevskyi VV, Pekhnyo VI, Vovk MV. Influence of synthesis conditions on complexation of Cu (II) with O, N, O tridentate hydrazone ligand. X-ray diffraction and spectroscopic investigations. J. Mol. Struct 2017;1146: 222-232.
https://doi.org/10.1016/j.molstruc.2017.05.140.
[52] Asadi Z, Golchin M, Eigner V, M, Amirghofran Z. A detailed study on the interaction of a novel water-soluble glycine bridged zinc(II) Schiff base coordination polymer with BSA: Synthesis, crystal structure, molecular docking and cytotoxicity effect against A549, Jurkat and Raji cell lines. Inorg.Chim.Acta 2017;465:50-60.
https://doi.org/10.1016/j.ica.2017.05.066.
[53] Sokolov FD, Brusko VV, Zabirov NG, Cherkasov RA. N-Acylamidophosphinates: Structure, Properties and ComplexationTowards Main Group Metal Cations. Curr. Org. Chem 2006;10:27-42.
[54] Wang D, Xing X, Ye X, Chen Z, Gou Z, Wu D. Synthesis, characterization and antibacterial activity of Zn(II) coordination polymer. J. Inorg. Biochem 2019;194:153-159.
https://doi.org/10.1016/j.jinorgbio.2019.02.014.
[55] Fleming I, Frontier Orbitals and Organic Chemical Reactions, Wiley, London, 1976.
[56] Kurtaran R, Odabasoglu S, Azizoglu A, Kara H, Atakol O. Experimental and computational study on [2,6-bis(3,5-dimethyl-N-pyrazolyl)pyridine]-(dithiocyanato)mercury(II). Polyhedron 2007;26:5069-5074.
https://doi.org/10.1016/j.poly.2007.07.021.
[57] Krogmann K. Die Kristallstruktur von $K_2[Pd(C_2O_4)_2]\cdot 4H_2O^{\dagger}$.ZACC 1966; 346:188-202.
https://doi.org/10.1002/zaac.19663460311.
[58] Otto S, Grabolle M, Forster C, Kreitner C, Resch-Genger U, Heinze K. $[Cr(ddpd)_2]^{3+}$: A Molecular, Water-Soluble, Highly NIR-Emissive Ruby Analogue. Angew. Chem. Int. Ed 2015; 54: 11572–11576.
https://doi.org/10.1002/anie.201504894.
[59] Andruh M, Melanson R, Stager CV, Rochon FD. $[Cr(bipy)(C_2O_4)_2]^-$—a versatile building block for the design of heteropolymetallic systems 2. Syntheses and crystal structures of - and $(AgCr(bipy)(\mu\text{-}C_2O_4)_2(H_2O)_2)_2$ and magnetic properties of the copper(II) derivative. Inorg.Chim.Acta 1996;251: 309-317.
https://doi.org/10.1016/S0020-1693(96)05284-X.
[60] Chohan ZH. Synthesis of Cobalt(II) and Nickel(II) Complexes of Ceclor (Cefaclor) and Preliminary Experiments on Their Antibacterial Character. Chem.Pharm. Bull 1991;39:1578-1580.
https://doi.org/10.1248/cpb.39.1578.
[61] Kilicasian D, Topal B D, Dolaz M, Golcu A, Ozkan SA. Synthesis, Characterization, Biological Activity and VoltammetricBehavior and Determination of Cefaclor Metal Complexes.Currenet.Anal.Chem 2010;6:316-328.
https://doi.org/10.2174/1573411011006040316.